

FIRST RELEASE OF HIGH REDSHIFT SUPERLUMINOUS SUPERNOVAE FROM  
THE SUBARU HIGH-Z SUPERNOVA CAMPAIGN (SHIZUCA).  
II. SPECTROSCOPIC PROPERTIES.

CHRIS CURTIN,<sup>1,2</sup> JEFF COOKE,<sup>1,2</sup> TAKASHI J. MORIYA,<sup>3,\*</sup> STEPHANIE R. BERNARD,<sup>4,2</sup> LLUÍS GALBANY,<sup>5</sup> JI-AN JIANG,<sup>6</sup>  
CHIEN-HSIU LEE,<sup>7</sup> KEIICHI MAEDA,<sup>8,9</sup> TOMOKI MOROKUMA,<sup>6</sup> KEN'ICHI NOMOTO,<sup>9</sup> GIULIANO PIGNATA,<sup>10,11</sup> TYLER PRITCHARD,<sup>1</sup>  
ROBERT M. QUIMBY,<sup>12,9</sup> NAO SUZUKI,<sup>9</sup> ICHIRO TAKAHASHI,<sup>9</sup> MASAYUKI TANAKA,<sup>3</sup> MASAOMI TANAKA,<sup>3</sup> NOZOMU TOMINAGA,<sup>13,9</sup>  
MASAKI YAMAGUCHI,<sup>6</sup> AND NAOKI YASUDA<sup>9</sup>

<sup>1</sup>Centre for Astrophysics & Supercomputing, Swinburne University of Technology, Hawthorn, VIC 3122, Australia

<sup>2</sup>ARC Centre of Excellence for All-Sky Astrophysics (CAASTRO)

<sup>3</sup>National Astronomical Observatory of Japan, National Institutes of Natural Sciences, 2-21-1 Osawa, Mitaka, Tokyo 181-8588, Japan

<sup>4</sup>School of Physics, University of Melbourne, Parkville VIC 3010, Australia

<sup>5</sup>PITT PACC, Department of Physics and Astronomy, University of Pittsburgh, Pittsburgh, PA 15260, USA

<sup>6</sup>Institute of Astronomy, Graduate School of Science, The University of Tokyo, 2-21-1 Osawa, Mitaka, Tokyo 181-0015, Japan

<sup>7</sup>Subaru Telescope, NAOJ, 650 N Aohoku Pl., Hilo, HI 96720, USA

<sup>8</sup>Department of Astronomy, Kyoto University, Kitashirakawa-Oiwake-cho, Sakyo-ku, Kyoto 606-8502, Japan

<sup>9</sup>Kavli Institute for the Physics and Mathematics of the Universe (WPI), The University of Tokyo Institutes for Advanced Study, The University of Tokyo, 5-1-5 Kashiwanoha, Kashiwa, Chiba 277-8583, Japan

<sup>10</sup>Departamento de Ciencias Físicas, Universidad Andres Bello, Avda. República 252, Santiago, 8320000, Chile

<sup>11</sup>Millennium Institute of Astrophysics (MAS), Nuncio Monseñor Sótero Sanz 100, Providencia, Santiago, Chile

<sup>12</sup>Department of Astronomy / Mount Laguna Observatory, San Diego State University, 5500 Campanile Drive, San Diego, CA, 92182-1221, USA

<sup>13</sup>Department of Physics, Faculty of Science and Engineering, Konan University, 8-9-1 Okamoto, Kobe, Hyogo 658-8501, Japan

ABSTRACT

We present Keck spectroscopic confirmation of three superluminous supernovae (SLSNe) at  $z = 1.851$ ,  $1.965$  and  $2.399$  detected as part of the Subaru High-Z sUpernova CAmpaign (SHIZUCA). The host galaxies have multi-band photometric redshifts consistent with the spectroscopic values. The supernovae were detected during their rise, allowing the spectra to be taken near maximum light. The restframe far-ultraviolet (FUV;  $\sim 1000\text{--}2500\text{\AA}$ ) spectra are made up in flux of approximately equal parts supernova and host galaxy. Weather conditions during observations were not ideal, and while the signal-to-noise ratios of the spectra are sufficient for redshift confirmation, the type of each event remains ambiguous. We compare our spectra to the few low redshift SLSN FUV spectra available to date and offer an interpretation as to the type of each supernova. We prefer SLSN-II classifications for all three events. The success of the first SHIZUCA Keck spectroscopic follow-up program is encouraging. It demonstrates that campaigns such as SHIZUCA are capable of identifying high redshift SLSNe with sufficient accuracy, speed and depth for rapid, well-cadenced and informative follow-up.

**Keywords:** methods: observational, (stars): supernovae: individual (SN-2016jhm, SN-2016jhn, SN-2017fei), galaxies: high-redshift, ultraviolet: general

## 1. INTRODUCTION

It is now known that some supernovae exceed an absolute magnitude of  $M \simeq -21$  (termed "superluminous supernovae"—SLSNe; Quimby et al. 2011; Gal-Yam 2012) and are luminous in the far-ultraviolet (FUV;  $\sim 1000\text{--}2500\text{\AA}$ ; Cooke et al. 2012; Yan et al. 2017a,c). SLSNe are exceedingly rare, occurring at  $\sim 0.001\times$  the frequency of general core-collapse supernovae (Quimby et al. 2013). But these transients promise to be powerful probes of the early universe, as they are already visible in ground based observations to redshifts of  $z = 4$  and greater (Cooke et al. 2012; Moriya et al. 2018; Mould et al. 2017).

Recent improvements to survey astronomy, such as large format CCD mosaics, have enabled more wide area surveys to operate, such as the Hyper Suprime-Cam Subaru Strategic Program (HSC-SSP; Aihara et al. 2017), the Dark Energy Survey (DES; Dark Energy Survey Collaboration et al. 2016), the Palomar Transient Factory (Law et al. 2009) and Pan-STARRS (Kaiser et al. 2010). These surveys monitor the vast amounts of sky required to detect SLSNe with a reasonable frequency. Additionally, these surveys are broad enough to allow boutique surveys such as the Subaru High-Z sUpernova CAmpaign (SHIZUCA; Moriya et al. 2018) and the Survey Using DECam for Superluminous Supernovae (SUDSS; Smith et al. 2016) to exercise more focused monitoring techniques and detect SLSNe with more efficiency.

There are advantages to surveying for SLSNe at high redshift ( $z \gtrsim 2$ ). Massive progenitors are invoked in all the explosion mechanisms used to explain SLSNe (Gal-Yam 2012), suggesting that the rate of SLSNe per unit volume varies with redshift similarly to the cosmic star formation rate, rising and perhaps peaking at  $z \sim 2$  (Madau & Dickinson 2014). This is consistent with rates measured up to this redshift (Prajs et al. 2017). Some if not all types of SLSNe show a preference for low metallicity hosts (Schulze et al. 2018) suggesting that the volumetric rate of SLSNe may continue to increase with redshift beyond the peak of star formation. The measured rate at  $z \sim 2\text{--}4$  is consistent with a continuing increase beyond  $z \sim 2$  (Cooke et al. 2012), though this measurement is very approximate.

Another advantage of looking to high redshift is the ability to sample the restframe FUV of SLSNe with optical facilities. As SLSNe are luminous in the FUV, this wavelength region contains valuable information about their explosion mechanisms (Mazzali et al. 2016). But FUV spectra of low redshift SLSNe can only be collected effectively from space-based telescopes, and so are taken infrequently. At high redshift this information is pushed into the optical bands, allowing for ground based observations.

High * ntendu* surveys like SHIZUCA are already capable of identifying supernovae to  $z > 4$  (Moriya et al. 2018). Spectroscopic follow-up of high redshift supernovae must be car-

ried out on 8m-class telescopes such as Keck due to their intrinsically faint apparent magnitudes (often  $m_r \gtrsim 24$  for  $z \gtrsim 2$ ).

Here we present spectra obtained with Keck of three high redshift SLSNe. This paper summarizes the first Keck spectroscopic follow-up program of SHIZUCA. We describe the observations in section 2. In section 3 we present the spectra and their redshift measurements. In section 4 we discuss our classification scheme and we present our conclusions in section 5. All calculations in this paper assume a  $\Lambda$ CDM cosmology with  $H_0 = 70\text{km s}^{-1} \text{Mpc}^{-1}$ ,  $\Omega_M = 0.3$  and  $\Omega_\Lambda = 0.7$ . All magnitudes are AB unless otherwise specified.

## 2. OBSERVATIONS

The COSMOS field (Scoville et al. 2007) of the HSC-SSP<sup>1</sup> supplies the photometry for this work and consists of a  $1.8 \text{ deg}^2$  field-of-view Hyper Suprime-Cam pointing imaged in five filters (*grizy*). The first SHIZUCA season was active on the COSMOS field from 2016 November to 2017 May. Further details of the SHIZUCA photometric analysis can be found in Moriya et al. (2018).

SHIZUCA uses COSMOS2015 photometric redshifts (Laigle et al. 2016) and MIZUKI redshifts (Tanaka 2015) to identify potential hosts of high redshift SLSNe from the HSC-SSP. The per-epoch depth of observation from the HSC-SSP using the 8.2m Subaru telescope ( $m_i \lesssim 26.5$ ) enables SHIZUCA to monitor the flux of high redshift sources in individual observing epochs. Any flux variations observed in these sources are then analyzed in the context of the photometric redshift of the host. Flux variations are identified as SLSN candidates using criteria such as non-recurrence, duration, light curve shape, peak magnitude and color evolution.

Follow-up spectroscopy of SHIZUCA high redshift SLSN candidates was acquired on 2016 December 28 and 2017 March 22–23 using the Low Resolution Imaging Spectrometer (LRIS; Oke et al. 1995; Steidel et al. 2004) on the Keck-I telescope. These data were obtained using the 400/3400 grism on the blue arm and the 400/8500 grating on the red arm separated at  $\sim 5600\text{\AA}$  using the D560 dichroic. The CCDs were read out using  $2\times 2$  binning with a spectral resolution of  $\sim 500\text{km s}^{-1}$ . The full width at half-maximum (FWHM) seeing ranged from  $0''.9\text{--}1''.1$ . During the March observations the blue shutter of LRIS failed and was fixed to remain open, and the trapdoor was used in its place. The spectra are made up of 1200s exposures on the blue side and 1179s exposures on the red side, with the difference chosen to allow the CCDs to finish reading out at the same time.

<sup>1</sup> General information for the HSC-SSP, such as location, cadence, and data products can be found at: <http://hsc.mtk.nao.ac.jp/ssp/> and the associated links.

For follow-up we selected SLSN candidates near maximum light with expected  $m_r \lesssim 25.5$  at the time of observation. The combined supernova and host continuum signal-to-noise (S/N) ratios near rest-frame 1500Å range from S/N  $\sim 3\text{--}5 \text{ pix}^{-1}$ . SLSNe usually arise in star-forming galaxies, such as Lyman break galaxies (LBGs), and this S/N is sufficient to reliably measure redshifts with strong UV absorption features from the interstellar medium (e.g., Steidel et al. 1998, 2003, 2004; Shapley et al. 2003; Cooke et al. 2006), along with Lyman- $\alpha$  (Ly- $\alpha$ ) emission when present and the Ly- $\alpha$  forest when visible.

From 6 candidates observed, three candidates arise in  $z > 1.8$  hosts which can be reliably matched with a LBG reference spectrum. Two candidates were identified as low redshift ( $z < 1$ ) and one did not have enough S/N for a confident redshift estimate. None of the candidates resembled other types of high redshift transients such as active galactic nuclei (AGN) or tidal disruption events (TDEs).

For the SLSN comparisons we use the FUV spectra of the SLSN-I SN2017egm (Quimby et al. 2017; Yan et al. 2017c), the SLSN-I Gaia16apd (Yan et al. 2017a) and the SLSN-II LSQ15abl (Quimby et al. 2015). These spectra were collected with the Hubble Space Telescope (HST) using the Cosmic Origins Spectrograph (COS; Shull 2009) and the Space Telescope Imaging Spectrograph (STIS; Woodgate et al. 1997). The reduced spectra are from the Mikulski Archive for Space Telescopes (MAST), and have been adjusted for scale and redshift as needed.

### 3. DATA REDUCTION AND ANALYSIS

#### 3.1. HSC16adga

HSC16adga (SN-2016jhm) was first detected by SHIZUCA on MJD 57715 at coordinates (RA, Dec) = (10:02:20.12, +02:48:43.4). The transient is detected in a star-forming host with a COSMOS photo- $z$  of  $2.26 \pm 0.3$  and a MIZUKI photo- $z$  peaking at 2.19. It is observed offset by  $0''.36$  ( $\sim 3\text{kpc}$ ) from the host galaxy flux centroid, helping to rule out an AGN or a TDE. The light curve of HSC16adga is shown in Figure 1.

We collected the Keck LRIS spectrum of HSC16adga on MJD 57751.09. From the light curve in Figure 1 the spectrum appears to have been taken near peak in the restframe UV. The spectrum, composed of 6 exposures (7200s blue, 7074s red), was reduced using standard IRAF procedures. The combined blue and red side 1-D spectrum is shown in Figure 2.

We identify a strong absorption feature at  $\sim 4100\text{\AA}$  with a slight flux break in the continuum at shorter wavelengths, which we attribute to Ly- $\alpha$  absorption and the Ly- $\alpha$  forest respectively. Applying these indicators as a first approximation of the redshift, we overlay the spectrum with a LBG composite. From the overlay several key ISM absorption features are apparent (e.g. SiII  $\lambda 1260$ , CII  $\lambda 1335$ , SiIV  $\lambda 1394$ , OIV]

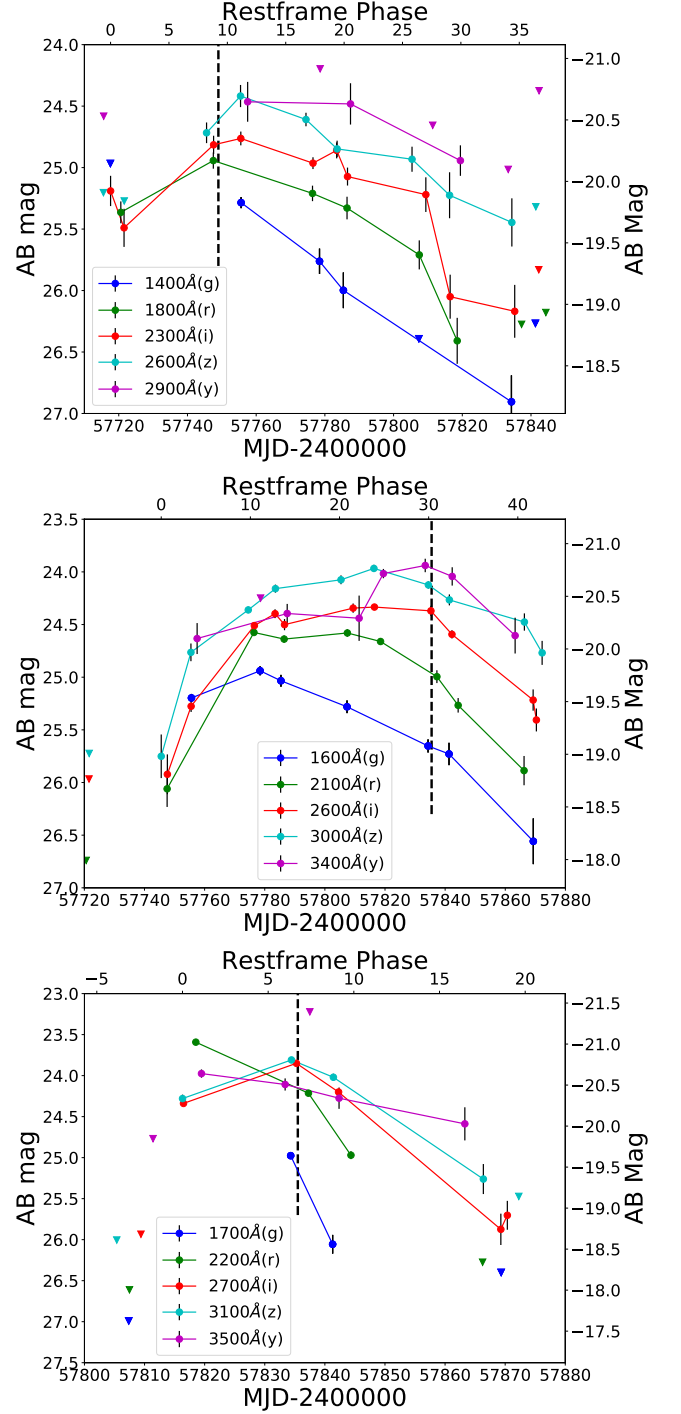


**Figure 1.** The HSC-*grizy* light curves of HSC16adga (top), HSC17auzg (middle) and HSC17dbpf (bottom). Triangles indicate upper limits and errors are  $1\sigma$ . The absolute magnitudes are calculated using  $z = 2.399, 1.965$  and  $1.851$  respectively, with a  $k$ -correction of  $2.5 \log(1+z)$ . The restframe timescales are relative to the dates of detection and the effective restframe wavelengths of the filters are given in the legends. Dates that spectra were acquired are identified by the vertical dashed black lines. See Moriya et al. (2018) for photometric methods.

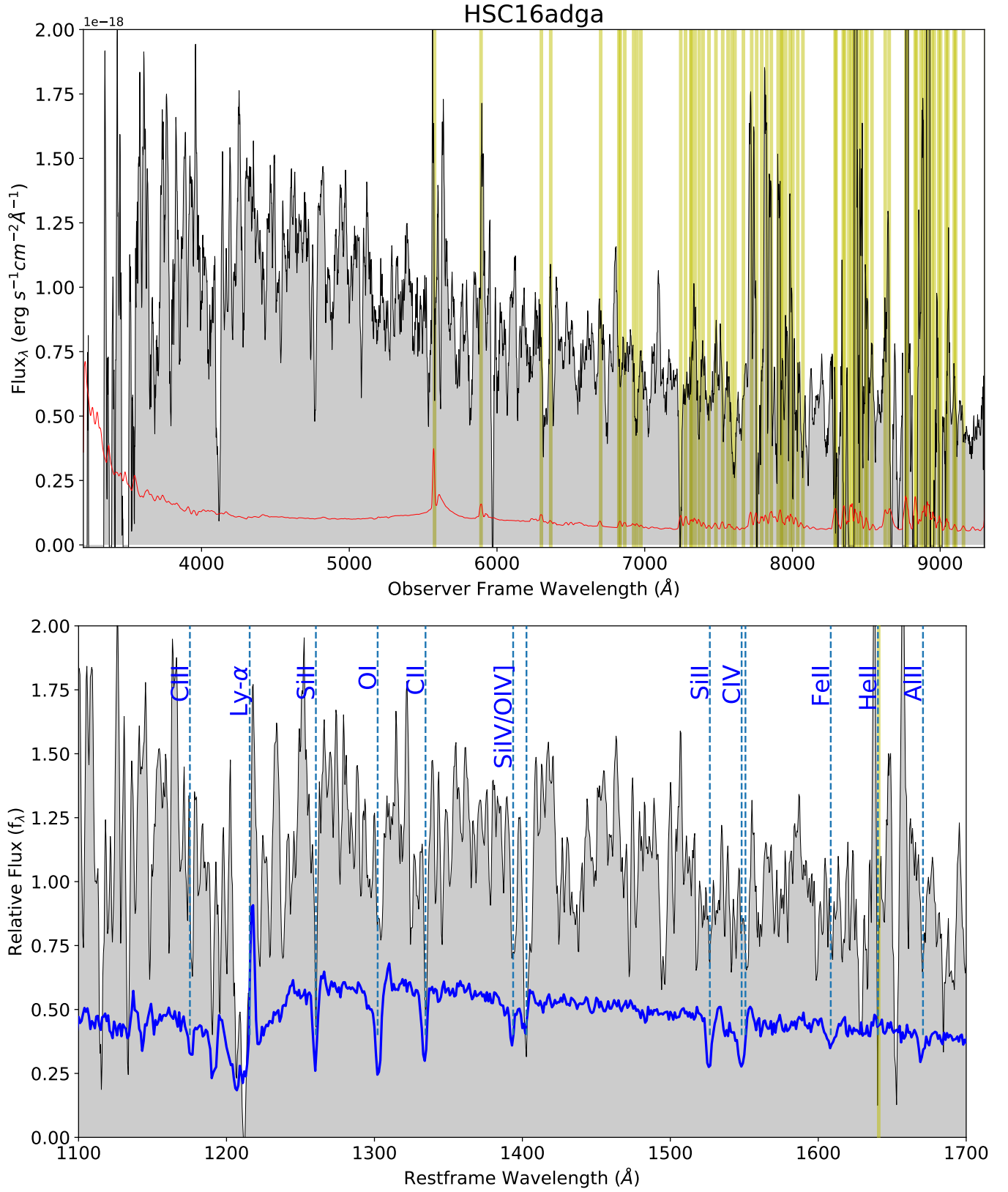


**Figure 2.** *Top:* Flux-calibrated observer-frame 1-D spectrum of HSC16adga, shown in black with grey fill. A 9 pixel boxcar smoothing function has been applied for clarity and to improve the S/N. The  $1\sigma$  boxcar<sup>-1</sup> error is shown in red. The spectrum is separated at  $5600\text{\AA}$  between the blue and red sides. The vertical yellow lines mark the locations of bright sky emission lines that are difficult to remove cleanly from faint spectra. *Bottom:* The same spectrum, zoomed-in and redshifted. A weak Ly- $\alpha$  absorber LBG composite spectrum is overlaid in blue and scaled arbitrarily to emphasize the alignment of features. A subset of the features used to constrain the redshift is illustrated with vertical dashed blue lines and labeled.



$\lambda 1403$ ), indicating a redshift of  $z = 2.399 \pm 0.004$  (see Figure 2).

### 3.2. HSC17auzg

HSC17auzg (SN-2016jhn) was first detected by SHIZUCA on MJD 57745 at coordinates (RA, Dec) = (09:59:00.42, +02:14:20.8). The transient is detected in a star-forming host with a COSMOS photo- $z$  of  $1.65 \pm 0.08$  and a MIZUKI photo- $z$  peaking at 1.78. It is observed offset by  $0''.78$  ( $\sim 6$ kpc) from the host galaxy flux centroid, helping to rule out an AGN or a TDE. The light curve of HSC17auzg is shown in Figure 1.

We collected the Keck LRIS spectrum of HSC17auzg on MJD 57835.80. From the light curve in Figure 1, we estimate that the spectrum was taken a few days to weeks after the restframe UV peak. The spectrum, composed of 7 exposures (8400s blue, 8253s red), was reduced using standard IRAF procedures. The 1-D spectrum is shown in Figure 3.

We identify a strong absorption feature at  $\sim 3500\text{\AA}$  which we attribute to Ly- $\alpha$ , enabling a first approximation of the redshift. An overlaid LBG composite spectrum reveals several key ISM absorption features (e.g. OI  $\lambda 1302$ , SiIV  $\lambda 1394$ , OIV]  $\lambda 1403$ , SiII  $\lambda 1527$ , CIV  $\lambda \lambda 1548, 1551$ , AlII  $\lambda 1671$ ), indicating a redshift of  $z = 1.965 \pm 0.004$  (see Figure 3).

### 3.3. HSC17dbpf

HSC17dbpf (SN-2017fei) was first detected by SHIZUCA on MJD 57816 at coordinates (RA, Dec) = (09:58:33.42, +01:59:29.7). The transient is detected in a star-forming host with a COSMOS photo- $z$  of  $2.25^{+0.1}_{-0.5}$  and a MIZUKI photo- $z$  peaking at 1.58. It is observed offset by  $0''.58$  ( $\sim 5$ kpc) from the host galaxy flux centroid, helping to rule out an AGN or a TDE. The light curve of HSC17dbpf is shown in Figure 1.

We collected two Keck LRIS spectra of HSC17dbpf on MJDs 57835.93 and 57836.84. The light curve in Figure 1 shows that the event evolved very quickly, so the peak is difficult to estimate. Still we suspect the spectrum was taken near the restframe UV peak. The spectra (see Figure 4) were taken over 2 consecutive nights treated as a single epoch, composed of 6 exposures (7200s blue, 7074s red).

The strong absorption feature at  $\sim 3400\text{\AA}$  we attribute to Ly- $\alpha$ . From a first approximation of the redshift, an overlaid LBG composite spectrum reveals several key ISM absorption features (e.g. OI  $\lambda 1302$ , CII  $\lambda 1335$ , SiIV  $\lambda 1394$ , OIV]  $\lambda 1403$ , SiII  $\lambda 1527$ , CIV  $\lambda \lambda 1548, 1551$ ), indicating a redshift of  $z = 1.851 \pm 0.004$  (see Figure 4).

## 4. DISCUSSION

The high FWHM seeing during observations resulted in the spectra having lower S/N than anticipated. As such while the supernova nature of each event is well supported, the specific type of each supernova remains unclear. Late-time

follow-up of the events would aid in determining their types, by enabling a more exact host galaxy subtraction, and because some SLSNe produce circumstellar emission features that become prominent at later times (Yan et al. 2017b; Fox et al. 2015).

The spectra confirm the high redshifts of the hosts, and though there are cases in which low redshift interlopers can mimic high redshift galaxy spectra, the MIZUKI photo- $z$  code shows only one peak in the redshift likelihood distribution for each host (Moriya et al. 2018). When the measured redshifts are applied to the photometry, light curves are produced in each case that are consistent with supernovae (Moriya et al. 2018). AGN and TDEs can sometimes resemble supernovae in their light curve behavior, but these are both highly centralized events, and our candidates are all significantly offset from their host galaxy flux centroids. Also, AGN usually exhibit strong emission lines in particular ratios (e.g. NV  $\lambda 1240$ , SiIV  $\lambda 1400$ , CIV  $\lambda 1550$ , CIII]  $\lambda 1909$ ; Vanden Berk et al. 2001) while TDEs are expected to have some HeII  $\lambda 1640$  emission (Arcavi et al. 2014). These features are not seen in any of our candidates.

SLSNe are often defined as supernovae that exceed an absolute AB magnitude of  $M = -21$  in any band (Gal-Yam 2012). However as the class has grown, the spectroscopic properties of different types of SLSNe have become more recognizable. When classifying SLSNe by their spectra, a continuum of peak magnitudes is observed for each type which extends fainter than  $M = -21$  (Rest et al. 2011; Nicholl et al. 2015; Lunnan et al. 2017). And while the first definition is self-consistent, the FUV peak magnitude distribution of SLSNe in relation to the optical peak magnitude distribution is largely unknown. Our supernovae are much brighter in the FUV than low redshift supernovae having FUV photometry that are not considered superluminous (Pritchard et al. 2014). As a result we classify the supernovae presented here as SLSNe.

### 4.1. Supernova Types

We attempt to discover the type each supernova by comparing the host-subtracted spectra to FUV spectra of low redshift SLSNe. There are currently only three low redshift SLSN FUV spectra available. Those are the SLSN-I SN2017egm (Quimby et al. 2017; Yan et al. 2017c), the SLSN-I Gaia16apd (Yan et al. 2017a), and the SLSN-II LSQ15abl (Quimby et al. 2015). We exclude the FUV spectrum of ASASSN-15lh because of the discrepancy arising as to its nature as a TDE (Leloudas et al. 2016). With so few spectra for comparison we attempt only to distinguish type-I events from type-II events.

Type-II supernovae are defined as those that exhibit hydrogen lines in spectra, typically H- $\alpha$  (Filippenko 1997). FUV spectra do not cover H- $\alpha$ , but type-IIs can also be confirmed

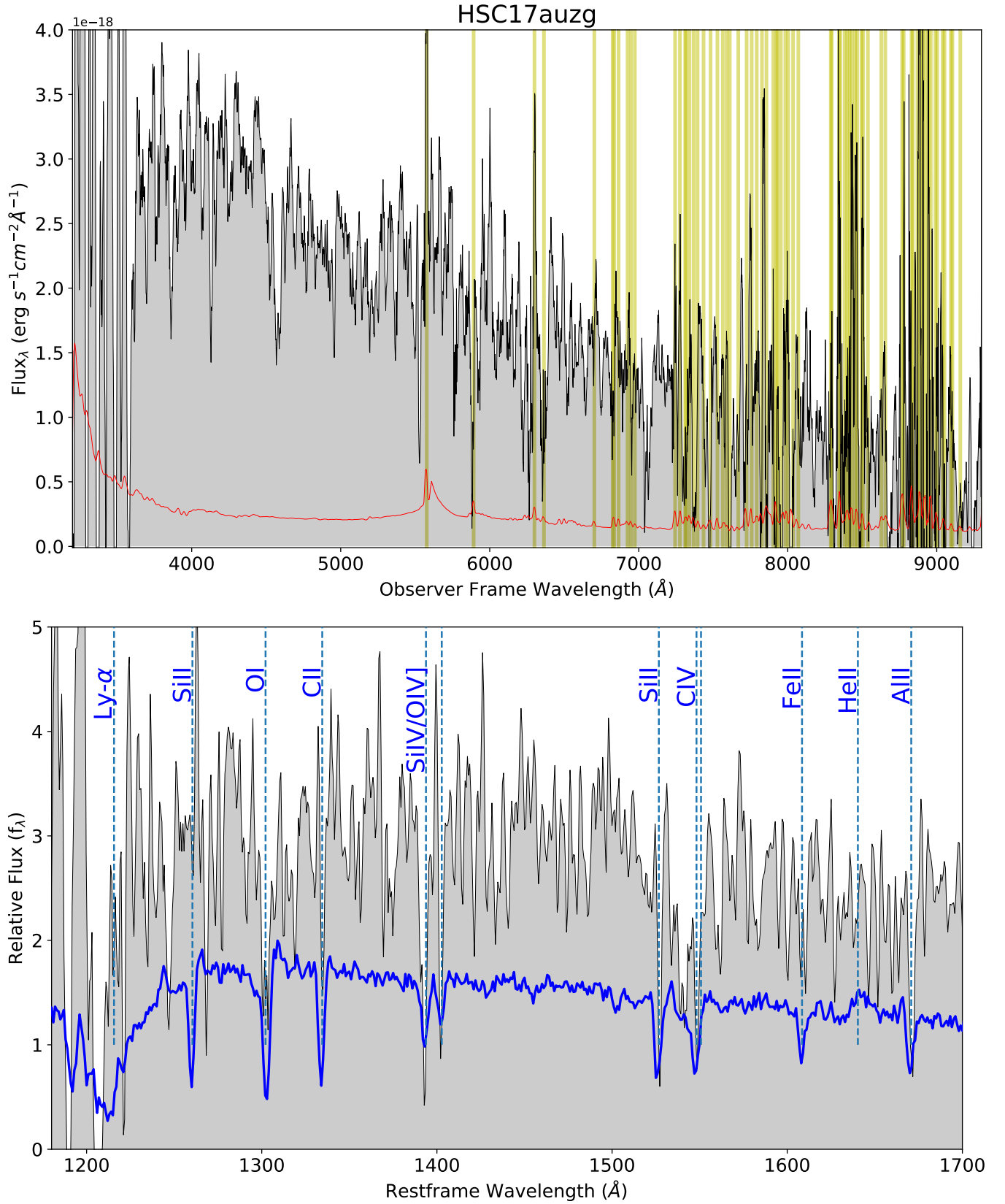


**Figure 3.** *Top:* Flux-calibrated observer-frame 1-D spectrum of HSC17auzg, similar to Figure 2. *Bottom:* The same spectrum, zoomed-in and redshifted similar to Figure 2. A strong Ly- $\alpha$  absorber LBG composite spectrum is overlaid in blue and scaled arbitrarily to emphasize the alignment of features. A subset of the features used to constrain the redshift is illustrated.

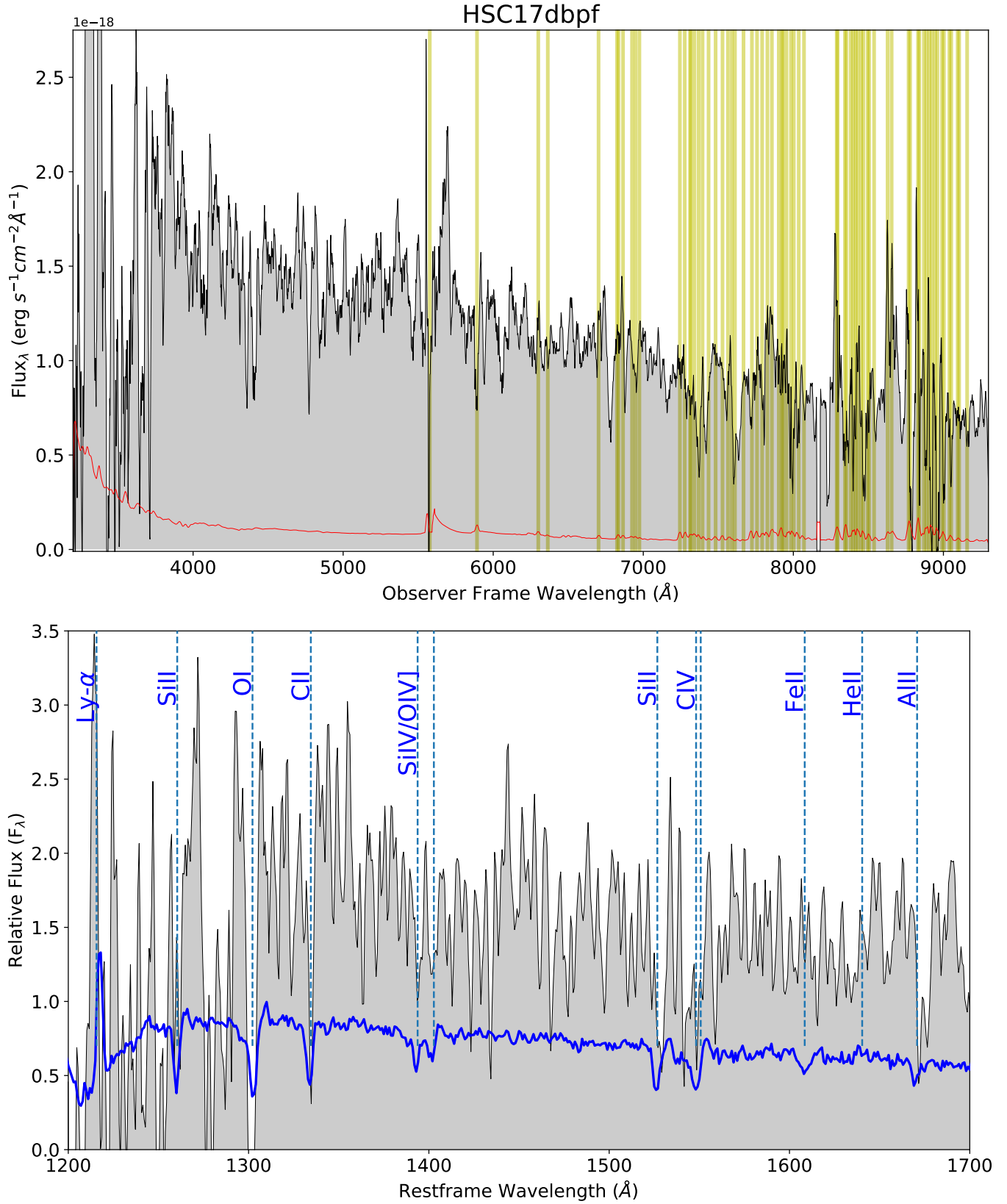


**Figure 4.** *Top:* Flux-calibrated observer-frame 1-D spectrum of HSC17dbpf, similar to Figure 2. *Bottom:* The same spectrum, zoomed-in and redshifted similar to Figure 2. A weak Ly- $\alpha$  absorber LBG composite spectrum is overlaid in blue and scaled arbitrarily to emphasize the alignment of features. A subset of the features used to constrain the redshift is illustrated.

with Ly- $\alpha$  emission (Fransson et al. 2005, 2014). LBGs, which are highly star-forming galaxies, are a common host type for high redshift supernovae (Cooke et al. 2009, 2012). However, they are also often strong Ly- $\alpha$  absorbers or emitters, which complicates the task of identifying supernova Ly- $\alpha$  emission.

Observed Ly- $\alpha$  emission in a high redshift supernova/host spectrum can still be used as a positive identifier of a type-II event if it can be confidently attributed to the supernova. In cases where the host and supernova are spatially separated on the sky enough that their profiles are distinguishable in observations, the source or sources of Ly- $\alpha$  emission can be seen directly. If this is not the case, the source of observed Ly- $\alpha$  emission can still be inferred from the characteristics of the feature. Ly- $\alpha$  emission from a supernova usually originates in the ejecta or a circum-stellar medium (CSM). Ly- $\alpha$  from ejecta is observed blueshifted from the host and broadened according to the ejecta temperature. Ly- $\alpha$  from a cold, slow moving CSM is observed as a narrow feature with a small velocity offset from the redshift of the host. In cases of LBGs with Ly- $\alpha$  in emission, the feature arises as Ly- $\alpha$  emission from the LBG is back-scattered off receding gas from outflows and passes back through the LBG off-resonance, avoiding absorption. Consequently, the feature is typically redshifted from the host by up to  $1000 \text{ km s}^{-1}$  or more (Shapley et al. 2003), making it distinguishable from supernova Ly- $\alpha$  emission.

Supernova Ly- $\alpha$  emission can also be completely absorbed by neutral hydrogen (HI) in the host interstellar medium (ISM), its circum-galactic medium (CGM), and the intervening intergalactic medium (IGM). Thus, the absence of observable supernova Ly- $\alpha$  emission does not necessarily rule out a type-II event. In cases where the lack of Ly- $\alpha$  emission is ambiguous, the presence of certain features unattributable to the host may be another reliable way to identify a SLSN-II from its FUV spectrum. In the case of LSQ15abl, the Ly- $\alpha$  feature has both narrow and intermediate components, indicating that at least some of this emission is from the supernova itself. LSQ15abl also exhibits several absorption features that are too broad to attribute to the host alone, and may be a blend of host and supernova absorption (see Figure 5). In addition, some SLSNe-II can be defined as SNe-II<sub>n</sub> (or SLSNe-II<sub>n</sub>) based on the presence of narrow emission lines (Smith & McCray 2007). Studies by Fransson et al. (2005, 2014) have shown that FUV spectra of some SNe-II<sub>n</sub> have signature features including emission and absorption. We use these SNe-II<sub>n</sub> signature lines, the common absorption transitions of LBGs from (Shapley et al. 2003), and the spectrum of LSQ15abl as a set of diagnostics for identifying broadened absorption.

The spectra of SLSNe-I have a number of characteristic broad features. The identification of several near-UV and op-

tical features (NUV; 2500–4000Å) as oxygen-II absorption which are common to SLSNe-I helped to define the class (Quimby et al. 2011). The broad features persist into the FUV (Yan et al. 2017a,c), though there are not yet enough FUV spectra to forecast whether these features are characteristic of SLSNe-I or whether their presence and strength correspond to other observables such as peak magnitude, rise time or evolutionary phase. Although the cause and atomic transitions responsible for the FUV absorption are not yet understood, the central wavelengths and widths of each feature appear uniform between the two low redshift FUV SLSN-I spectra currently available (see Figure 5). This uniformity holds true for broad features observed in the optical, for which there are many more SLSN-I spectra available. If confirmed with additional data, it is possible that SLSN-I may be classified via their FUV broad absorption alone.

Because we do not have spectra of the host galaxies alone, we perform a “pseudo-host” subtraction on each spectrum to aid our analysis. We assume a LBG-like host for each supernova, consistent with the templates used for the photometric redshift estimates (Moriya et al. 2018). Analyses of a large sample of LBGs Shapley et al. (2003); Cooke et al. (2009) show that the characteristics and color of a LBG spectrum are strongly correlated with the equivalent width of the Ly- $\alpha$  feature. Shapley et al. (2003) divided their sample into equivalent width quartiles and constructed composite spectra for each. The quartiles are referred to here as strong Ly- $\alpha$  absorbers, weak Ly- $\alpha$  absorbers, weak Ly- $\alpha$  emitters and strong Ly- $\alpha$  emitters. We include these composites in our pseudo-host construction, using the estimated absorption or emission strength of Ly- $\alpha$  from the host of each event to respectively select the specific composite to use for subtraction.

To accurately scale the pseudo-hosts, we calculate the ratio of host flux to supernova flux (as measured most closely in time to our observations) in each spectrum using the associated HSC photometry (Moriya et al. 2018). The high-redshift hosts are near-point sources and the bulk of the flux enters the spectroscopic slit. However we centered the slits on the supernovae, thus some of the host flux may not be included. When necessary we apply a geometrical correction to account for any portion of the host not within the spectroscopic slit.

The wavelength range of the spectra include the HSC-*gri* bands. To construct the pseudo-hosts over this whole range, we use the LBG composite spectra from 912–2000 Å (their full extent) and starburst (SB) templates from Calzetti et al. (1994) at wavelengths beyond 2000Å. Ly- $\alpha$  absorbers have redder UV continua compared to Ly- $\alpha$  emitters (Shapley et al. 2003; Cooke et al. 2009). We therefore use the SB2 template ( $0.10 < E(B-V) < 0.21$ ) to complete a pseudo-host constructed with a Ly- $\alpha$  absorber LBG composite, and we



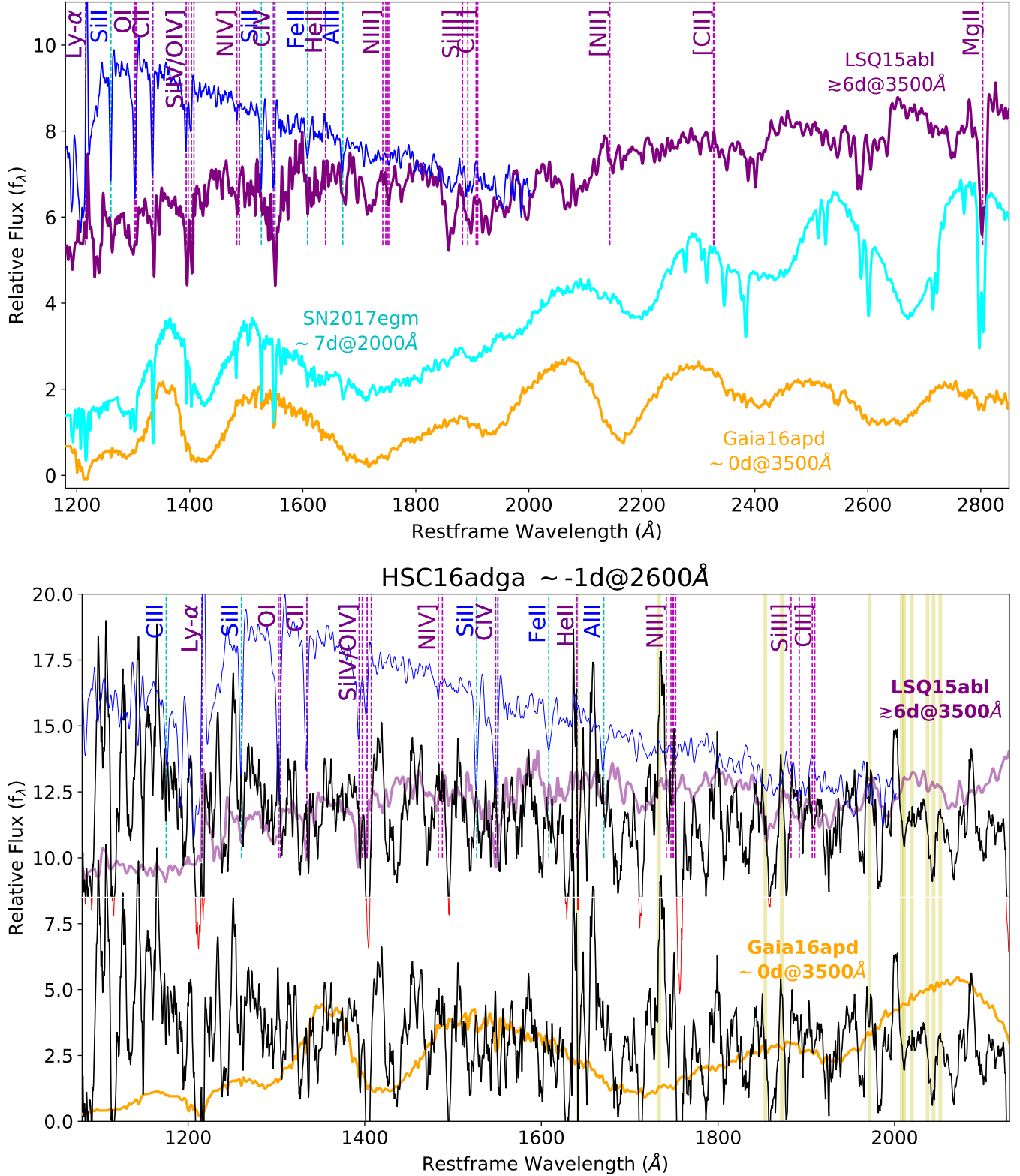


**Figure 5. Top:** FUV spectra of low redshift SLSNe. The orange and cyan spectra are SLSNe-I and the purple spectrum is a SLSN-II. A LBG composite spectrum is shown in blue for comparison of the absorption features seen in the SLSN-II to those commonly seen in star-forming hosts alone. The vertical dashed blue lines mark absorption features of LBGs identified in (Shapley et al. 2003), and the magenta lines mark absorption and emission features of SNe-II identified in Fransson et al. (2005, 2014). Lines in common between SNe-II and LBGs have been deferred to magenta. **Bottom:** The pseudo-host subtracted spectrum of HSC16adga (black/red). The spectrum is displayed twice to simplify the comparison to the low redshift FUV SLSN spectra. It is shown in red in regions where the pseudo-host subtraction has produced negative flux. The overlaid spectra are from the top figure and have the same color scheme. The LBG composite used for subtraction is shown in blue. Features are identified as in the top figure.

use the SB1 template ( $E(B-V) < 0.10$ ) to complete a pseudo-host constructed with a Ly- $\alpha$  emitter LBG composite.

#### 4.1.1. *HSC16adga*

To produce the pseudo-host subtracted spectrum of HSC16adga we use a weak Ly- $\alpha$  absorber LBG composite with a SB2 tail. The supernova spectrum (see Figure 5) is the bluest of the three here and bluer than the low redshift comparison spectra. This spectrum was acquired early in the UV peak and the blueness may be due to an unusually high early-time temperature (estimated  $\gtrsim 20000\text{K}$ , [Moriya et al. 2018](#)).

The effect of the Ly- $\alpha$  forest is weaker than expected at wavelengths shortward of  $1216\text{\AA}$  as is apparent by comparing the spectrum to the LBG composite used for subtraction which includes a redshift based average Ly- $\alpha$  forest decrement. However, we have no photometric information for the supernova in this wavelength region, and cannot ensure that the pseudo-host does not underestimate the flux here. This is also the point at which the uncertainty in the flux measured by LRIS is rising rapidly, and the region which requires the largest correction during flux calibration. A better host subtraction is needed before speculating further.

The supernova spectrum of HSC16adga does not exhibit any obvious Ly- $\alpha$  emission and so cannot be classified as a SLSN-II outright. Though as discussed earlier, we cannot rule out that Ly- $\alpha$  emission from the explosion is being absorbed by environmental HI. However there are several typical host absorption features that appear broadened, most notably OI  $\lambda 1302$  which is broader in both LSQ15abl and HSC16adga than is typically seen in LBG spectra. Additionally, the complex appearance of the blended SiIV/OIV  $\lambda\lambda 1394, 1397, 1403, 1407$  feature could arise from narrow absorption from the host inscribed onto broad emission from the supernova. The broadened emission is seen in SNe-IIn ([Fransson et al. 2005, 2014](#)), though in this case the significance is too low to confirm. Finally, the coarse blackbody shape of the overall spectrum is consistent with a bluer LSQ15abl-like object.

There is some resemblance between the supernova spectrum of HSC16adga and that of the SLSN-I, Gaia15apd. Most of the continuum peaks are present (e.g.  $1360\text{\AA}$ ,  $1510\text{\AA}$ ,  $1880\text{\AA}$ ), and the continuum slopes in the proximity of the peaks are also in relative agreement. But there is no strong evidence for the broad absorption features that are seen in the two low redshift SLSN-I FUV comparison spectra (e.g.  $1290\text{\AA}$ ,  $1420\text{\AA}$ ,  $1710\text{\AA}$ ). However, it may be that the features are present but weaker than those seen in the comparison spectra, and the S/N is too low to detect them. More spectra of  $z > 2$  SLSNe in the future, and with higher S/N, will establish the relative strengths to expect of the various absorption features, and enable more confident classification.

Our analysis suggests that the behavior of HSC16adga is more indicative of a SLSN-II rather than a SLSN-I. At a redshift of 2.399, this is the highest redshift supernova ever spectroscopically observed near peak.

#### 4.1.2. *HSC17auzg*

HSC17auzg is offset from its host enough that a significant fraction of the flux from the host is not included in the spectral slit. By projecting the slitmask onto a contour plot of the host, we estimate that only  $\sim 50\%$  of the host flux is being observed in each of the  $g$ ,  $r$  and  $i$  bands. The photometric estimate of the host contribution to the spectrum used to scale the pseudo-host for subtraction has been adjusted accordingly. We use as a pseudo-host of HSC17auzg a strong Ly- $\alpha$  absorber LBG composite spectrum with a SB2 tail.

The differenced supernova spectrum of HSC17auzg (see Figure 6) is similar in color to LSQ15abl, more so than the bluer HSC16adga. This is not surprising given that the spectrum is from a phase of the supernova later than that of HSC16adga and similar or slightly earlier than that of LSQ15abl. Even so, all three spectra are consistent with relatively smooth blackbodies at different temperatures.

Like HSC16adga, HSC17auzg exhibits several typical host absorption features that appear broadened. Most notable are OI  $\lambda 1302$  and, as is also seen in LSQ15abl, CIV  $\lambda 1548$ .

There is a prominent emission feature centered at  $\lambda 1196$  which could be attributed to moderately broad/blueshifted Ly- $\alpha$  emission from the supernova heavily absorbed by HI from the host but partially escaping via a clumpy medium. This is consistent with the pseudo-host being best fit by a strong Ly- $\alpha$  absorber LBG composite. The  $\lambda 1196$  feature is strong, with  $S/N \sim 10$  compared to  $S/N \sim 3$  for that of the surrounding continuum flux of the supernova-host combined spectrum. However, it is unclear from the 2-D spectrum if the feature is an artifact of the CCD and more pronounced in the 1-D extraction. Also, the feature is seen in the same problematic wavelength range discussed in the analysis of HSC16adga, where the uncertainty in the flux measured by LRIS is rising rapidly and the largest adjustments are applied to the flux during calibration. If the feature is associated with Ly- $\alpha$ , it indicates that HSC17auzg is a SLSN-II by definition. However, a better host subtraction or evidence of time-dependent evolution in the feature is needed before speculating further.

There is little resemblance between the supernova spectrum of HSC17auzg and that of the SLSN-I, Gaia15apd. There is the minimal likeness of the  $1510\text{--}1710\text{\AA}$  peak-trough feature, but the other relevant absorption features ( $1290\text{\AA}$ ,  $1420\text{\AA}$ ,  $2180\text{\AA}$ ) are absent.

Our analysis suggests that the behavior of the supernova spectrum of HSC17auzg is more indicative of a SLSN-II event rather than a SLSN-I event. This type assignment can

be confirmed if the feature at  $1196\text{\AA}$  is verified as emission from the supernova.

#### 4.1.3. *HSC17dbpf*

The blue side of the spectrum of HSC17dbpf has a flatter continuum slope than HSC16adga or HSC17auzg (see Figure 4). We suspect this behavior may be due to systematics in the observations rather than a difference in the nature of the event. The apparent bump in the spectrum at  $\sim 5500\text{\AA}$ , observer-frame, seems to arise as a consequence of the spectrum being constructed with exposures taken over two consecutive nights. The exposures were precisely aligned before stacking, but a loss of tracking on the second night allowed the object to drift towards the edge of the slit. The effect of this drift on the calibration of the spectrum is large enough to account for the observed flattening.

To produce the pseudo-host subtracted spectrum of HSC17dbpf we use a weak Ly- $\alpha$  absorber LBG composite with a SB2 tail (see Figure 6). The supernova spectrum appears quite red despite being acquired very near the UV peak, though rapid cooling is not unexpected given the unusually fast evolution of the event. The redness is consistent with the estimated temperature of the event at this phase ( $\sim 14000\text{K}$ , Moriya et al. 2018).

The subtraction produces a large flux deficit at  $\sim 1250\text{\AA}$  (displayed in red in the figure). This feature is seen in the same highly suspect wavelength region described in the analyses of HSC16adga and HSC17auzg. Again, we have no photometric information for the supernova in this region, and cannot ensure that the pseudo-host subtraction is accurate; this is the point at which the uncertainty in the flux measured by LRIS is rising rapidly and the region which requires the largest correction during flux calibration. Thus we reserve judgment on features and behaviors observed at these wavelengths.

There is a flux spike at  $1213\text{\AA}$  in the vicinity of Ly- $\alpha$ , but given the caveats associated with this wavelength region of the spectrum, this feature cannot be considered significant. If the spike can be verified as Ly- $\alpha$  emission with a better host subtraction or evidence of time-dependent evolution, it indicates that HSC17dbpf is a SLSN-II by definition.

The supernova spectrum of HSC17dbpf does not exhibit any broadened absorption or broad emission with inscribed narrow host absorption – features like those seen in HSC16adga and HSC17auzg and typical of type-II supernovae in general. Still, the shape of the spectrum as that of a coarse blackbody is not uncharacteristic of SLSNe-II, as is evidenced by the very similar overall continuum behavior between HSC17dbpf and LSQ15abl.

The spectrum of HSC17dbpf does not exhibit any of the broad absorption features observed in the spectra of Gaia16apd and SN2017egm.

Our analysis suggests that the behavior of the supernova spectrum of HSC17dbpf is not inconsistent with a SLSN-II event but is highly uncharacteristic of a SLSN-I event. A SLSN-II classification can be verified if the feature at  $1213\text{\AA}$  is validated as emission from the supernova.

## 5. CONCLUSION

With this SHIZUCA pilot spectroscopic follow-up program we have demonstrated the feasibility of spectroscopic follow-up of high redshift SLSNe, testing the current limits of high redshift transient spectral analysis. The high étendu and dense cadence of the HSC-SSP combined with the detection efficiency of SHIZUCA can generate high redshift SLSN candidates at a sufficient rate to statistically enable follow-up of several targets near maximum light at any time during an active observation campaign. Keck LRIS provides the best facility for spectroscopic follow-up of  $z \sim 2$  supernovae in terms of light gathering power combined with blue sensitivity.

We have reported on FUV spectroscopic follow-up of three SLSNe at  $z = 1.851$ ,  $1.965$  and  $2.399$ , including the highest redshift supernova ever spectroscopically observed near peak. The spectra are extracted from  $\sim 2$  hour exposures taken under sub-optimal seeing conditions. The S/N of the reduced spectra are relatively low, and flux measurements become unreliable at wavelengths shortward of  $3500\text{\AA}$ . Thus, in spectra with similar S/N, moderate to weak Ly- $\alpha$  features cannot be confirmed at  $z \lesssim 2$ . However, analyses can be extended to lower wavelengths in spectra with higher S/N.

Our analysis of the pseudo-host subtracted supernova spectra suggests that all three events are most likely to be SLSNe-II, though none can be confirmed via confident identification of supernova Ly- $\alpha$  emission. Although none of the spectra exhibit the broad absorption features indicative of SLSNe-I, the S/N of the spectra may be too low to detect them. We estimate that doubling the S/N of the spectra presented here would enable supernova type confirmations of future events. By observing under optimal seeing conditions, employing longer exposures and perhaps taking advantage of brighter than average targets, this S/N is achievable.

Future follow-up is merited, to ascertain if any of the supernovae exhibit late-time strong emission from which type information can be inferred, such as Ly- $\alpha$  emission like that reported in Yan et al. (2017b). Additionally, late-time spectra of the hosts with little to no supernova contribution can be used to produce more exact host subtracted supernova spectra and better constrain the UV continuum, enabling further analysis.

Observed Ly- $\alpha$  emission associated with a high redshift supernova can be used to confirm a type-II classification. However, given that hosts of high redshift SNe are often Ly- $\alpha$  absorbers, the absence of Ly- $\alpha$  emission in a supernova spec-

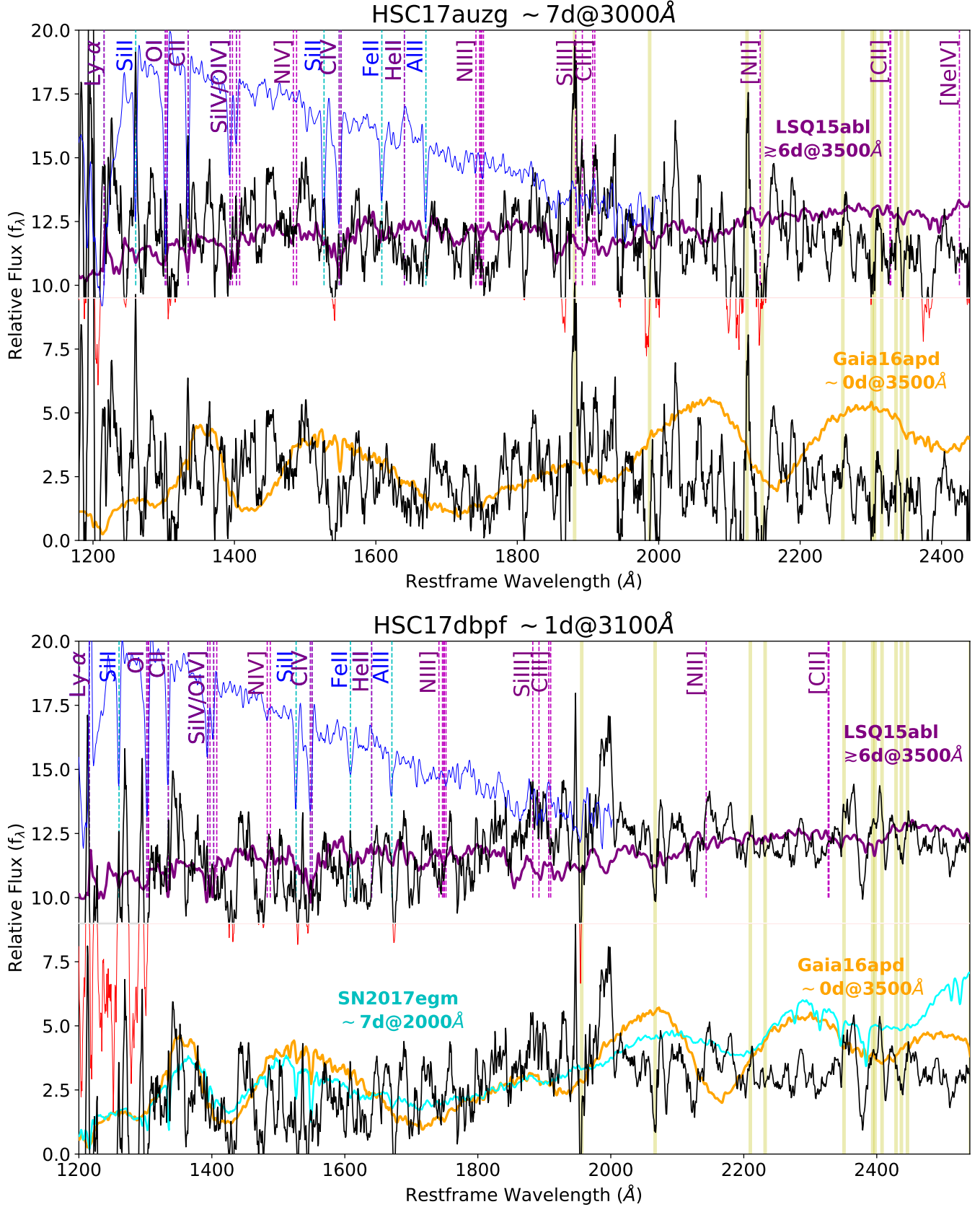


**Figure 6.** *Top:* The pseudo-host subtracted spectrum of HSC17auzg, as in Figure 5. *Bottom:* The host subtracted spectrum of HSC17dbpf, as in Figure 5.



trum may be due to absorption by environmental H I and cannot be used to rule out a type-II event. In such cases there are other potential type-II indicators to infer the classification. The low redshift FUV spectrum of LSQ15abl exhibits broadened absorption that cannot be attributed to the host alone. SNe-II<sub>n</sub>, which can manifest as SLSNe-II, can exhibit a variety of broad emission features (i.e. OII  $\lambda$ 1302, NIV]  $\lambda$ 1486, NIII]  $\lambda$ 1750, CIII]  $\lambda$ 1909, [Fransson et al. 2005](#)). A spectroscopic time series may be an effective way to identify type-II events suffering strong Ly- $\alpha$  host absorption by revealing an evolution in Ly- $\alpha$  emission more identifiable than the emission itself. The accuracy of these methods can be tested with spectra of confirmed high redshift SNe-II.

There are  $\sim 10$  photometric supernova and SLSN candidates from SHIZUCA at  $z \sim 2$  and higher redshifts. More spectra are needed to confirm candidates and develop the accuracy of photometric confirmation. With a sufficient number of confident events, precise rates of SLSNe by type and redshift can be established. This will be explored in a future paper. However, an approximate rate calculation discussed in ([Moriya et al. 2018](#)) of  $z \sim 2$  SLSNe based on the events presented here is consistent with previous findings ([Cooke et al. 2012](#)) and the expectation that the rate of SLSNe per unit volume is higher at high redshift.

SHIZUCA is capable of detecting events to  $z > 6$ , and with the right observing strategy and clear skies, spectroscopic follow-up of these events out to the edge of the epoch of reionization may be achievable. And the potential of the James Webb Space Telescope will be much greater, capable of acquiring spectra of SLSNe as far as  $z = 20$ . At such high redshifts, only deep, wide-field infrared surveys will be capable of producing targets. Such surveys are already being considered with future facilities such as the University of Tokyo Atacama Observatory (TAO) and the Kunlun Dark Universe Survey Telescope (KDUST). By exploring the current limits of high redshift transient astronomy, SHIZUCA and similar programs are setting the stage for observing the explosions of the very first stars.

## ACKNOWLEDGEMENTS

This research is supported by the Grants-in-Aid for Scientific Research of the Japan Society for the Promotion of Science (TJM 16H07413, 17H02864) and by JSPS Open Partnership Bilateral Joint Research Project between Japan and Chile.

C.C. would like to express his appreciation to Uros Mestric for all his assistance with the observations and the data analysis.

J.C. acknowledges the Australian Research Council Future Fellowship grant FT130101219.

L.G. was supported in part by the US National Science Foundation under Grant AST-1311862.

Support for G.P. is provided by the Ministry of Economy, Development, and Tourism’s Millennium Science Initiative through grant IC120009, awarded to The Millennium Institute of Astrophysics, MAS. G.P. also acknowledges support by the Proyecto Regular FONDECYT 1140352.

This research is partly supported by Japan Science and Technology Agency CREST JPMHCR1414.

Parts of this research were conducted by the Australian Research Council Centre of Excellence for All-sky Astrophysics (CAASTRO), through project number CE110001020.

The Hyper Suprime-Cam (HSC) collaboration includes the astronomical communities of Japan and Taiwan, and Princeton University. The HSC instrumentation and software were developed by the National Astronomical Observatory of Japan (NAOJ), the Kavli Institute for the Physics and Mathematics of the Universe (Kavli IPMU), the University of Tokyo, the High Energy Accelerator Research Organization (KEK), the Academia Sinica Institute for Astronomy and Astrophysics in Taiwan (ASIAA), and Princeton University. Funding was contributed by the FIRST program from Japanese Cabinet Office, the Ministry of Education, Culture, Sports, Science and Technology (MEXT), the Japan Society for the Promotion of Science (JSPS), Japan Science and Technology Agency (JST), the Toray Science Foundation, NAOJ, Kavli IPMU, KEK, ASIAA, and Princeton University.

The Pan-STARRS1 Surveys (PS1) have been made possible through contributions of the Institute for Astronomy, the University of Hawaii, the Pan-STARRS Project Office, the Max-Planck Society and its participating institutes, the Max Planck Institute for Astronomy, Heidelberg and the Max Planck Institute for Extraterrestrial Physics, Garching, The Johns Hopkins University, Durham University, the University of Edinburgh, Queen’s University Belfast, the Harvard-Smithsonian Center for Astrophysics, the Las Cumbres Observatory Global Telescope Network Incorporated, the National Central University of Taiwan, the Space Telescope Science Institute, the National Aeronautics and Space Administration under Grant No. NNX08AR22G issued through the Planetary Science Division of the NASA Science Mission Directorate, the National Science Foundation under Grant No. AST-1238877, the University of Maryland, and Eotvos Lorand University (ELTE).

This paper makes use of software developed for the Large Synoptic Survey Telescope. We thank the LSST Project for making their code available as free software at <http://dm.lsst.org>.

Based on data collected at the Subaru Telescope and retrieved from the HSC data archive system, which is operated by the Subaru Telescope and Astronomy Data Center at National Astronomical Observatory of Japan.



Based in part on data obtained at the Gemini Observatory via the time exchange program between Gemini and the Subaru Telescope processed using the Gemini IRAF package (program ID: S17A-056, GS-2017A-Q-13). The Gemini Observatory is operated by the Association of Universities for Research in Astronomy, Inc., under a cooperative agreement with the NSF on behalf of the Gemini partnership: the National Science Foundation (United States), the National Research Council (Canada), CONICYT (Chile), Ministerio de Ciencia, Tecnología e Innovación Productiva (Argentina), and Ministério da Ciência, Tecnologia e Inovação (Brazil).

This research has made use of the NASA/IPAC Extragalactic Database (NED) which is operated by the Jet Propulsion Laboratory, California Institute of Technology, under con-

tract with the National Aeronautics and Space Administration.

Some of the data presented in this paper were obtained from the Mikulski Archive for Space Telescopes (MAST). STScI is operated by the Association of Universities for Research in Astronomy, Inc., under NASA contract NAS5-26555. Support for MAST for non-HST data is provided by the NASA Office of Space Science via grant NNX09AF08G and by other grants and contracts.

Support for *HST* program GO-13784 was provided by NASA through a grant from the Space Telescope Science Institute, which is operated by the Association of Universities for Research in Astronomy, Inc., under NASA contract NAS 5-26555.

*Facilities:* Keck/LRIS, Subaru/HSC, Gemini/GMOS-S

## REFERENCES

- Aihara, H., Armstrong, R., Bickerton, S., et al. 2017, ArXiv e-prints, [arXiv:1702.08449 \[astro-ph.IM\]](#)
- Arcavi, I., Gal-Yam, A., Sullivan, M., et al. 2014, [ApJ](#), **793**, 38
- Calzetti, D., Kinney, A. L., & Storchi-Bergmann, T. 1994, [ApJ](#), **429**, 582
- Cooke, J., Sullivan, M., Barton, E. J., et al. 2009, [Nature](#), **460**, 237
- Cooke, J., Wolfe, A. M., Gawiser, E., & Prochaska, J. X. 2006, [ApJ](#), **652**, 994
- Cooke, J., Sullivan, M., Gal-Yam, A., et al. 2012, [Nature](#), **491**, 228
- Dark Energy Survey Collaboration, Abbott, T., Abdalla, F. B., et al. 2016, [MNRAS](#), **460**, 1270
- Filippenko, A. V. 1997, [ARA&A](#), **35**, 309
- Fox, O. D., Smith, N., Ammons, S. M., et al. 2015, [MNRAS](#), **454**, 4366
- Fransson, C., Challis, P. M., Chevalier, R. A., et al. 2005, [ApJ](#), **622**, 991
- Fransson, C., Ergon, M., Challis, P. J., et al. 2014, [ApJ](#), **797**, 118
- Gal-Yam, A. 2012, [Science](#), **337**, 927
- Kaiser, N., Burgett, W., Chambers, K., et al. 2010, in [Proc. SPIE](#), Vol. 7733, [Ground-based and Airborne Telescopes III](#), 77330E
- Laigle, C., McCracken, H. J., Ilbert, O., et al. 2016, [ApJS](#), **224**, 24
- Law, N. M., Kulkarni, S. R., Dekany, R. G., et al. 2009, [PASP](#), **121**, 1395
- Leloudas, G., Fraser, M., Stone, N. C., et al. 2016, [Nature Astronomy](#), **1**, 0002
- Lunnan, R., Chornock, R., Berger, E., et al. 2017, ArXiv e-prints, [arXiv:1708.01619 \[astro-ph.HE\]](#)
- Madau, P., & Dickinson, M. 2014, [ARA&A](#), **52**, 415
- Mazzali, P. A., Sullivan, M., Pian, E., Greiner, J., & Kann, D. A. 2016, [MNRAS](#), **458**, 3455
- Moriya, T. J., Tanaka, M., Yasuda, N., et al. 2018, [ApJ](#), submitted
- Mould, J., Abbott, T., Cooke, J., et al. 2017, [Science Bulletin](#), Volume 62, Issue 10, pp. 675-678, **62**, 675
- Nicholl, M., Smartt, S. J., Jerkstrand, A., et al. 2015, [MNRAS](#), **452**, 3869
- Oke, J. B., Cohen, J. G., Carr, M., et al. 1995, [PASP](#), **107**, 375
- Prajs, S., Sullivan, M., Smith, M., et al. 2017, [MNRAS](#), **464**, 3568
- Pritchard, T. A., Roming, P. W. A., Brown, P. J., Bayless, A. J., & Frey, L. H. 2014, [ApJ](#), **787**, 157
- Quimby, R. M., Cooke, J., Brown, P. J., et al. 2017, The Astronomer's Telegram, 1050
- Quimby, R. M., Cooke, J., & Pritchard, T. 2015, The Astronomer's Telegram, 7439
- Quimby, R. M., Yuan, F., Akerlof, C., & Wheeler, J. C. 2013, [MNRAS](#), **431**, 912
- Quimby, R. M., Kulkarni, S. R., Kasliwal, M. M., et al. 2011, [Nature](#), **474**, 487
- Rest, A., Foley, R. J., Gezari, S., et al. 2011, [ApJ](#), **729**, 88
- Schulze, S., Krühler, T., Leloudas, G., et al. 2018, [MNRAS](#), **473**, 1258
- Scoville, N., Aussel, H., Benson, A., et al. 2007, [ApJS](#), **172**, 150
- Shapley, A. E., Steidel, C. C., Pettini, M., & Adelberger, K. L. 2003, [ApJ](#), **588**, 65
- Shull, J. M. 2009, in [American Institute of Physics Conference Series](#), Vol. 1135, [American Institute of Physics Conference Series](#), ed. M. E. van Steenberg, G. Sonneborn, H. W. Moos, & W. P. Blair, 301
- Smith, M., Sullivan, M., D'Andrea, C. B., et al. 2016, [ApJL](#), **818**, L8
- Smith, N., & McCray, R. 2007, [ApJL](#), **671**, L17
- Steidel, C. C., Adelberger, K. L., Dickinson, M., Giavalisco, M., & Pettini, M. 1998, ArXiv Astrophysics e-prints, [astro-ph/9812167](#)

- Steidel, C. C., Adelberger, K. L., Shapley, A. E., et al. 2003, [ApJ](#), 592, 728
- Steidel, C. C., Shapley, A. E., Pettini, M., et al. 2004, [ApJ](#), 604, 534
- Tanaka, M. 2015, [ApJ](#), 801, 20
- Vanden Berk, D. E., Richards, G. T., Bauer, A., et al. 2001, [AJ](#), 122, 549
- Woodgate, B. E., Kimble, R. A., Bowers, C. W., et al. 1997, in [Proc. SPIE](#), Vol. 3118, *Imaging Spectrometry III*, ed. M. R. Descour & S. S. Shen, 2
- Yan, L., Quimby, R., Gal-Yam, A., et al. 2017a, [ApJ](#), 840, 57
- Yan, L., Lunnan, R., Perley, D. A., et al. 2017b, [ApJ](#), 848, 6
- Yan, Y., Pereley, D., De Cia, A., et al. 2017c, ArXiv e-prints, [arXiv:1711.01534v1 \[astro-ph\]](#)